References

[1] Brogan, F. and Almroth, B. O., "Buckling of Cylinders with Cutouts," *AIAA Journal*, Vol. 8, No. 2, Feb. 1970, pp. 236–240.

[2] Stricklin, J. A. et al., "Linear and Nonlinear Analysis of Shells of Revolution with Asymmetric Stiffness Properties," *Proceedings of the Second Conference on Matrix Methods of Structural Mechanics*, AFFDL TR-69, Oct. 1968, Wright-Patterson Air Force Base, Ohio.

[3] Marlowe, M. B. and Flügge, W., "Some New Developments in the Foundations of Shell Theory," LMSC-6-78-68-13, May 1968, Lockheed Missiles & Space Company, Palo Alto, Calif.

[4] Sanders, J. L., Jr., "Nonlinear Theories for Thin Shells," *Quarterly of Applied Mathematics*, Vol. 21, No. 1, 1963, pp. 21–36.

[5] Kempner, J. and Chen, Y.-N., "Buckling and Postbuckling of an Axially Compressed Oval Cylindrical Shell," *Symposium on the Theory of Shells to Honor Lloyd Hamilton Donnell*, McCutchan Publishing Corp., Univ. of Houston, May 1967, pp. 141–183; also PIBAL Rept. 917, Polytechnic Institute of Brooklyn.

[6] Kempner, J. and Chen, Y.-N., "Postbuckling of an Axially Compressed Oval Cylindrical Shell," *Proceedings of the 12th International Congress of Applied Mechanics*, Aug. 26–31, 1968, Stanford Univ., Palo Alto, Calif., pp. 246–268; also PIBAL Rept. 68-31, Polytechnic Institute of Brooklyn.

JANUARY 1971 AIAA JOURNAL VOL. 9, NO. 1

Cylindrical Shell with an Axisymmetric Moving Load

K. SCHIFFNER*

Institut für Festigkeit, Deutsche Forschungs-und Versuchsanstalt für Luft-und Raumfahrt E.V., Mülheim/Ruhr, Germany

AND

C. R. STEELE†

Stanford University, Palo Alto, Calif.

The transient response of a semi-infinite, simply-supported cylindrical shell caused by an axisymmetrically engulfing, step pressure wave is investigated. Equations including the effects of transverse shear deformtion and rotary inertia are used. The rather involved contour integral solution to the problem is evaluated by means of modified saddle-point methods in terms of the Fresnel integrals and the integral of the Airy function. As expected, for load velocities smaller than the shear wave velocity of the shell material, the cylinder response is found to be analogous to that for an Euler-Bernoulli beam on an elastic foundation. Thus a load velocity equal to the minimum phase velocity is a "critical" velocity; i.e., the response increases with the square root of the distance of the load front from the end of the cylinder and, so, can become of large magnitude for practical problems of long cylinders with little damping. For the high load velocities, the short wavelength portion of the response is analogous to that for a Timoshenko beam on an elastic foundation, for which no further "critical" velocities occur, even at the "shear" and "bar"—which for the cylinder becomes the "plate"—velocities. However, in the long wavelength portion of the response of the cylinder, the transition from "bending" to axial "membrane" behavior causes the "bar" velocity to also be critical.

Introduction

PROBLEMS involving the transient response of structures to moving loads have attracted a number of investigators who have utilized various approaches. However, for the long cylinder the direct finite element, finite difference, or modal superposition numerical methods are not advantageous because of the localized nature of the transient response. To take advantage of this nature, the relatively simple "steady-state" solution, which depends only on the distance from a moving load discontinuity, has been utilized, as in the investigations by Jones and Bhuta,[1] and Herrmann and Baker.[2] This steady-state solution indicates that unbounded response occurs at four "critical" load speeds. These are equal to 1) the speed of disturbance propagation in a flat plate, 2) the slightly lower speed of propagation in a bar, 3) the speed of shear waves, and 4) the substantially lower minimum phase velocity for the cylinder.

In order to understand the significance of the steady-state solution in general and the actual behavior at the critical load speeds in particular, the transient response of the semi-infinite beam on an elastic foundation, which is analogous to the cylinder in many respects, was investigated. In Ref. 3, the response of the Euler-Bernoulli beam was found to increase with the square root of the distance of the load discontinuity from the beam end when the load speed equaled the minimum phase velocity, which qualifies this load speed to be referred to as critical. However, in the investigation of the Timoshenko beam,[4] it was found that, although the solution never achieves a "steady-state," the response to a load moving at the shear and bar velocities was bounded; so these speeds are not actually critical.

Thus, with a background of work on the analogous, but considerably simpler beam problems, we come to the present task of investigating the transient response of the cylinder. In particular, we seek a resolution to the question of which of the four speeds, at which the steady-state solution does not exist, are actually critical load speeds.

Since the high load speeds are of interest, equations including the effect of transverse shear deformation and rotary iner-

Presented as Paper 70-18 at the AIAA 8th Aerospace Sciences Meeting, New York, January 19–21, 1970; submitted November 7, 1969; revision received May 4, 1970.

* Abteilungsleiter, Abteilung Statik und Dynamik; NASA University Fellow for 1968/69 at Stanford University.

† Associate Professor of Aeronautics and Astronautics. Stanford University. Member AIAA.

tia are used, as in[2] and in the investigations by Naghdi and Cooper.[5,6] The straight-forward Fourier integral solution is modified to contour integrals for which various saddlepoint methods are applicable. The results are asymptotically valid when either the time and/or space variable is sufficiently large. This is of course the region of greatest interest, since the response is small near the simply-supported end when the load first moves on the cylinder. The asymptotic methods used are: 1) the usual saddlepoint expansion,[7] 2) the Fresnel integral solution when a pole of the integrand is near the saddlepoint,[8,9] 3) the Airy function solution when two saddlepoints are near each other, discussed in Ref. 9, and 4) a result, obtained in this investigation, in terms of an integral of the Airy function for the case when two saddlepoints and a pole of any order are adjacent.

Formulation of the Problem

We consider a cylindrical shell of constant thickness h and radius a, which is axisymmetrically loaded by a radial pressure step-load moving with constant velocity v_0 in the axial direction along the shell. The deformations, strains and stresses of the cylinder are assumed to be symmetric with respect to the axis of revolution. With the usual assumptions of the theory of thin shells, the governing equations which include the effects of transverse shear deformation and rotary inertia may be written as follows.[2,5,6] The equations of equilibrium are

$$\partial N_x/\partial x = \rho h(\partial^2 u/\partial t^2) + \rho(h^3/12a)\partial^2\psi/\partial t^2 \quad (1a)$$

$$\partial V_x/\partial x - N_\theta/a = \rho h\partial^2 w/\partial t^2 + q \quad (1b)$$

$$\partial M_x/\partial x - V_x = \rho(h^3/12)[\partial^2\psi/\partial t^2 + (1/a)\partial^2 u/\partial t^2] \quad (1c)$$

and the stress-displacement relations are

$$N_x = [Eh/(1-\nu^2)][\partial u/\partial x + \nu w/a + (h^2/12a)\partial\psi/\partial x] \quad (2a)$$

$$N_\theta = [Eh/(1-\nu^2)](w/a + \nu\partial u/\partial x) \quad (2b)$$

$$M_x = [Eh^3/12(1-\nu^2)][\partial\psi/\partial x + (1/a)\partial u/\partial x] \quad (2c)$$

$$V_x = \kappa Gh[\partial w/\partial x + \psi] \quad (2d)$$

The quantities N_x, N_θ are stress resultants in the axial and circumferential direction, M_x the resultant moment and V_x the resultant transverse shear force, as shown in Fig. 1. The axial and radial displacements are u and w; ψ is the change of slope of the normal to the middle surface; ρ, E, G, ν are the mass density, modulus of elasticity, shear modulus, and Poisson's ratio. The constant κ is given in Refs. 5, 6 as

$$\kappa = \kappa_1 E/G(1-\nu^2) \text{ with } \kappa_1 = \nu \quad (3)$$

which gives $\kappa = \frac{5}{6}$. When $\nu = 0.3$. The pressure step-load is given by

$$q(x,t) = \begin{cases} 0 & x > v_0 t \\ q_0 & x < v_0 t \end{cases} \quad (4)$$

For a semi-infinite cylindrical shell, which is simply supported on the finite end, the boundary conditions may be written as

$$N_x = 0, \quad w = 0, \quad M_x = 0: \quad \text{at } x = 0 \quad (5)$$

With respect to these boundary conditions, it is useful to express the system of Eqs. (1) and (2) in terms of strains ϵ_x, ϵ_θ and curvature κ_x‡

$$\begin{bmatrix} \frac{\partial^2}{\partial x^2} - \gamma^2\frac{\partial^2}{\partial t^2} & \nu\frac{\partial^2}{\partial x^2} & 0 \\ \frac{\nu}{a} & \frac{1}{a} - \kappa_1 a\frac{\partial^2}{\partial x^2} + \gamma^2 a\frac{\partial^2}{\partial t^2} & -\kappa_1 \\ 0 & -a\kappa_1\frac{\partial^2}{\partial x^2} & -\kappa_1 + \frac{h^2}{12}\left(\frac{\partial^2}{\partial x^2} - \gamma^2\frac{\partial^2}{\partial t^2}\right) \end{bmatrix} \begin{bmatrix} \epsilon_x \\ \epsilon_\theta \\ \kappa_x \end{bmatrix} = \begin{bmatrix} 0 \\ -q\frac{1-\nu^2}{Eh} \\ 0 \end{bmatrix} \quad (6)$$

‡ For a detailed derivation of these equations see Ref. 12.

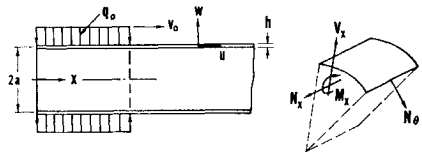

Fig. 1 Shell geometry.

where the usual expression for axial strain is modified by the term $(h^2/12a)\partial\psi/\partial x$ and terms of order $h^2/12a^2$ are neglected in comparison to 1

$$\kappa_1 - \nu h^2/12a^2 \approx \kappa_1$$
$$1 - h^2/12a^2 \approx 1 \quad (7)$$

This system of equations has the same form as the approximate system of equations of motion for cylindrical shells given by Naghdi and Cooper.[5,6] But it describes both the phase velocities and the ratios of amplitudes of displacements (strains, curvature) in good agreement with the results found for the "more exact" equations also discussed in Refs. 5 and 6. When we replace u, the displacement in the axial direction, by a modified displacement u^*, $u^* = u + (h^2/12a)\psi$, it is not necessary to neglect the middle surface strains in the moment resultant relation Eq. 2 and the terms involving $h^2/12a$ in Eqs. (1) and (2), as done in Refs. 5 and 6, to evaluate the approximate system of equations (II) in Ref. 5. The only necessary simplification is that given in Eq. (7). When u is replaced by u^*, the differences in the ratios of displacement amplitudes found in Ref. 5 for the "exact" equations and the approximate system of equations do not occur. Next, the following variables

$$x = \xi a, \quad \epsilon_x = p_0\epsilon_\xi, \quad v = v_0\gamma \quad (8a)$$

$$t = \gamma a\tau, \quad \epsilon_y = p_0\epsilon_\eta, \quad p_0 = q_0\, a(1-\nu^2)/Eh \quad (8b)$$

$$\alpha = 12a^2/h^2\kappa_1, \quad \kappa_x = p_0/a\kappa_\xi, \quad p = -q/q_0 \quad (8c)$$

are introduced into Eq. (6) to obtain a system of equations in dimensionless form

$$\begin{bmatrix} \frac{\partial^2}{\partial\xi^2} - \frac{\partial^2}{\partial\tau^2} & \nu\frac{\partial^2}{\partial\xi^2} & 0 \\ \nu & 1 - \kappa_1\frac{\partial^2}{\partial\xi^2} + \frac{\partial^2}{\partial\tau^2} & -\kappa_1 \\ 0 & -\alpha\frac{\partial^2}{\partial\xi^2} & -\alpha + \left(\frac{\partial^2}{\partial\xi^2} - \frac{\partial^2}{\partial\tau^2}\right) \end{bmatrix} \times \boldsymbol{\epsilon} = \begin{bmatrix} 0 \\ p \\ 0 \end{bmatrix} \quad (9)$$

with the boundary conditions at $\xi = 0$

$$\boldsymbol{\epsilon} = \mathbf{0} \quad (10)$$

where

$$\boldsymbol{\epsilon} = \begin{bmatrix} \epsilon_\xi \\ \epsilon_\eta \\ \kappa_\xi \end{bmatrix}$$

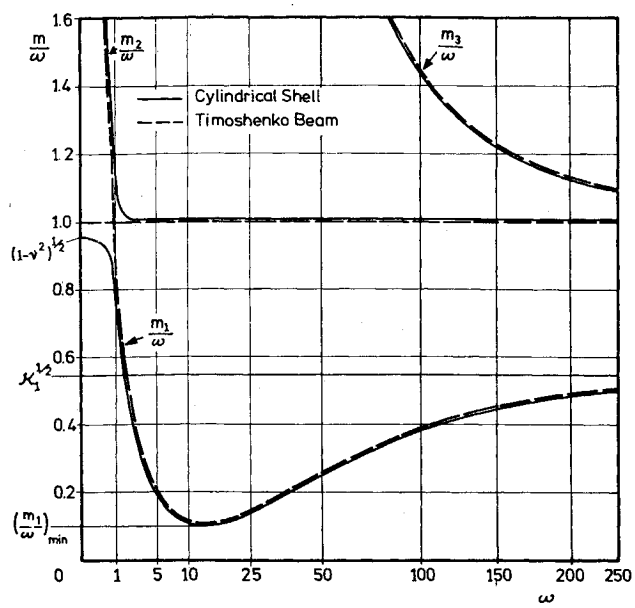

Fig. 2 Phase velocities for an isotropic cylindrical shell with $\nu = 0.3$, $\eta_1 = 0.3$, $h/a = 0.02$ ($\alpha = 0.9 \times 10^4$).

and p the pressure step-load distribution

$$p = \begin{cases} 0 & \text{when} \quad \xi > v\tau \\ 1 & \text{when} \quad \xi < v\tau \end{cases} \tag{11}$$

We assume the cylindrical shell is initially in rest and undeformed; thus

$$\boldsymbol{\varepsilon} = (\partial/\partial t)\boldsymbol{\varepsilon} = 0 \qquad \tau \leq 0 \tag{12}$$

A further simplification, neglecting the effects of transverse shear deformation and rotary inertia to obtain a system of equations corresponding to Donnell's equations, would lead to a system of differential equations with different order of derivatives with respect to time "τ" and space "ξ." Such a system is not hyperbolic; so strains, stresses and displacements do not vanish for points ahead of all the wave fronts.

The system Eq. (8) is uncoupled for $\nu = 0$. Then the equations involving ϵ_η and $\varkappa_\xi$ correspond exactly to the equations for the Timoshenko beam on an elastic foundation investigated in Ref. 4, while the remaining equation gives the axial motion-identically zero for the present problem.

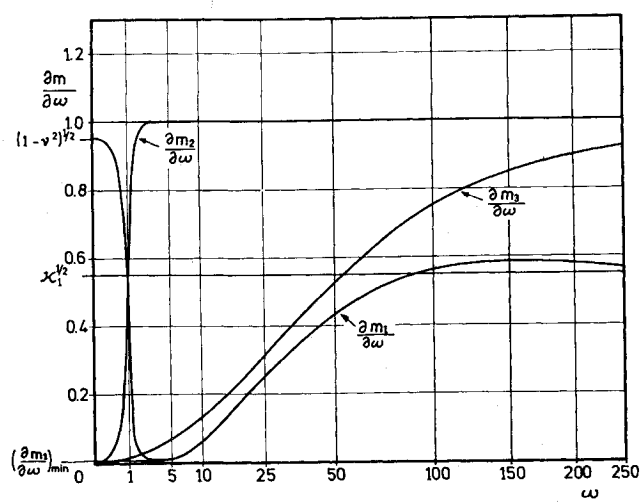

Fig. 3 Group velocities for an isotropic cylindrical shell with $\nu = 0.3$, $\eta_1 = 0.3$, $h/a = 0.02$ ($\alpha = 0.9 \times 10^4$).

General Solution

Since the differential system Eq. (9) contains only derivatives of even order and the boundary conditions are of the form Eq. (10), the Fourier sine transform technique will be used to determine the strain vector $\boldsymbol{\varepsilon}$.

The solution for the transformed strain vector $\boldsymbol{\varepsilon}^{(s)}$, which is defined by

$$\boldsymbol{\varepsilon}^{(s)}(\omega\tau) = \int_0^\infty \boldsymbol{\varepsilon}(\xi,\tau)\, \sin(\omega\xi)d\xi \tag{13a}$$

$$\boldsymbol{\varepsilon}(\xi,\tau) = \frac{2}{\pi}\int_0^\infty \boldsymbol{\varepsilon}^{(s)}(\omega,\tau)\, \sin(\omega\xi)d\omega \tag{13b}$$

may be written in the form

$$\boldsymbol{\varepsilon}^{(s)} = \sum_1^3 \mathbf{b}_k \cos m_k\tau + \mathbf{b}_v \cos\omega v\tau + \mathbf{b}_0 \tag{14}$$

where

$$\mathbf{b}_1 = \frac{1}{\omega(m_1^2 - m_2^2)(m_3^2 - m_1^2)}\left[\frac{1}{(\omega v)^2 - m_1^2} + \frac{1}{m_1^2}\right] \times \begin{bmatrix} -\nu\omega^2(\alpha + \omega^2 - m_1^2) \\ (\alpha + \omega^2 - m_1^2)(\omega^2 - m_1^2) \\ \alpha\omega^2(\omega^2 - m_1^2) \end{bmatrix}$$

and $\mathbf{b}_2$, $\mathbf{b}_3$ are given by cyclic interchanging of indices 1–3

$$\mathbf{b}_v = \frac{1}{\omega[(\omega v)^2 - m_1^2][(\omega v)^2 - m_2^2][(\omega v)^2 - m_3^2]} \times \begin{bmatrix} -\nu\omega^2[\alpha + \omega^2(1 - \nu^2)] \\ [\alpha + \omega^2(1 - \nu^2)]\omega^2(1 - \nu^2) \\ \alpha\omega^4(1 - \nu^2) \end{bmatrix}$$

$$\mathbf{b}_0 = -\mathbf{b}_v(v = 0) = \frac{1}{\omega m_1^2 m_2^2 m_3^2}\begin{bmatrix} -\nu\omega^2(\alpha + \omega^2) \\ (\alpha + \omega^2)\omega^2 \\ \alpha\omega^4 \end{bmatrix}$$

Equation (14) satisfies the differential Eq. (9) in transformed form and the initial condition Eq. (12). The functions $m_1(\omega)$, $m_2(\omega)$, $m_3(\omega)$ are three independent roots (the other three are $-m_1$, $-m_2$, $-m_3$) of the polynomial

$$m^6 - m^4[(2 + \kappa_1)\omega^2 + (\alpha + 1)] + m^2[(2\kappa_1 + 1)\omega^4 + (\alpha + 2 - \nu^2)\omega^2 + \alpha] - \omega^2[\kappa_1\omega^4 + (1 - \nu^2)\omega^2 + \alpha(1 - \nu^2)] = 0 \tag{15}$$

corresponding to a solution for traveling waves in the form[5]

$$\boldsymbol{\varepsilon} = \mathbf{c}e^{i(m\tau - \omega\xi)}$$

where the transform variable ω is the dimensionless wave number and m the frequency. Introducing the phase velocities $(m/\omega)_k$, (see Ref. 5), Eq. (15) can be reduced to a quadratic equation in ω^2:

$$\omega^4\left[\left(\frac{m}{\omega}\right)^2 - 1\right]^2\left[\left(\frac{m}{\omega}\right)^2 - \kappa_1\right] - \omega^2\left[\left(\frac{m}{\omega}\right)^2 - 1\right] \times \left[(\alpha + 1)\left(\frac{m}{\omega}\right)^2 - (1 - \nu^2)\right] + \alpha\left[\left(\frac{m}{\omega}\right)^2 - (1 - \nu^2)\right] - 0 \tag{16}$$

The poles of ω^2 are at $(m/\omega)^2 = 1$ and $(m/\omega)^2 = \kappa_1$ which give the "plate" and "shear wave" velocities, respectively. A zero occurs at

$$(m/\omega)^2 = 1 - \nu^2$$

The minimum phase velocity is determined to be

$$(m/\omega)^2_{\min} = (4(1 - \nu^2)\kappa_1/\alpha)^{1/2} - [(1 - \nu^2) + 2\kappa_1]/\alpha + 0(\alpha^{-3/2}) \tag{17}$$

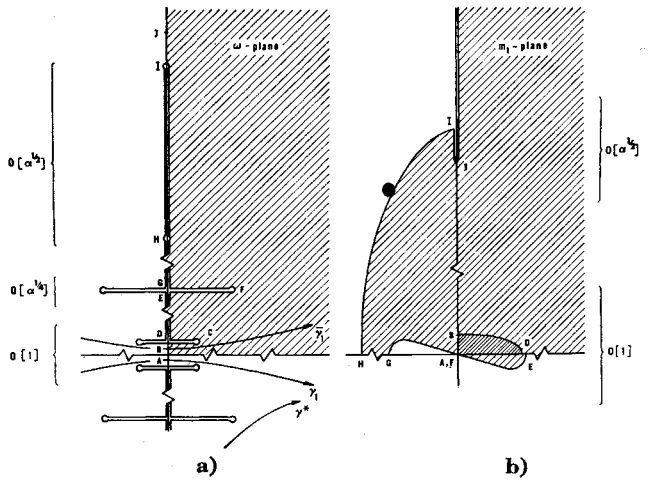

Fig. 4 Conformal mapping of the first quadrant of the ω plane on the m_1-plane.

that is, at the wave number

$$\omega^2 = \left(\frac{1-\nu^2}{\kappa_1}\alpha\right)^{1/2} + \frac{1}{\kappa_1}[(1-\nu^2) + \kappa_1(1-2\nu^2)] + 0(\alpha^{-1/2}) \quad (18)$$

For positive real values of ω, the phase velocities are shown in Fig. 2. For comparison, the phase velocities for the Timoshenko beam on an elastic foundation are plotted as they are found from Eq. (16) with $\nu = 0$ (see also Ref. 4). The Timoshenko beam seems to be a useful model describing the dynamical behavior of an axisymmetric deformed cylindrical shell when the wave number ω is larger than $\alpha^{1/4}$. The group velocities which are defined as $(\partial m/\partial\omega)_\varkappa$ may be easily obtained for given values of ω and $(m/\omega)_\varkappa$ by differentiation of Eq. (16) with respect to ω. Figure 3 shows the group velocities for a cylindrical shell.

Since the inversion Fourier sine integral Eq. (13) will be shifted to a complex integration contour, the behavior of m_1, m_2, m_3, in the complex plane must be clarified. The usual method of solving the third order polynomial in m^2 Eq. (15) results in an eighth order polynomial of ω whose roots are branchpoints of $m(\omega)$.

This polynomial has four roots of the magnitude $\omega = 0(1)$, approximately given by

$$b_{12} = [(1-\nu^2)^{1/2} + i\nu][1 + 0(\alpha^{-1})]; \quad -b_{12};\ \bar{b}_{12};\ -\bar{b}_{12} \quad (19)$$

and four roots of the magnitude $\omega = 0(\alpha^{1/2})$

$$b_{31} = [1/(1-\varkappa_1^{1/2})]i[\alpha^{1/2} + 0(\alpha^{-1/2})]; \ -b_{31} \quad (20a)$$

$$b_{32} = [1/(1+\varkappa_1^{1/2})]i[\alpha^{1/2} + 0(\alpha^{-1/2})]; \ -b_{32} \quad (20b)$$

For the indices k,l in b_{kl} note that at $\omega = b_{lk}$

$$m_1(b_{lk}) = m_k(b_{lk})$$

Branchpoints also occur at the zeros of $m_1(\omega)$ ($m_2(\omega)$ and $m_3(\omega)$ have no zeros) which are approximately evaluated as

$$b_{11} = \frac{1+i}{2^{1/2}}\left(\frac{\alpha}{\kappa_1}(1-\nu^2)\right)^{1/4} \times \left[1 + \frac{i}{4}\left(\frac{1-\nu^2}{\kappa_1}\right)^{1/2}\alpha^{-1/2} + 0(\alpha^{-1})\right] - \quad -b_{11};\ \bar{b}_{11};\ -\bar{b}_{11} \quad (21)$$

In order to make $m_1(\omega)$, $m_2(\omega)$, and $m_3(\omega)$ single valued in the complex ω-plane and analytic on and near the entire real axis, the branchcuts are chosen as indicated in Figs. 4a, 5a, and 6b, where the points $\omega = b_{12};\ b_{11};\ b_{31};\ b_{13}$ are denoted by C,F,H,I, respectively. Figures 4b, 5b, and 6b show the mapping of the first quadrant of the ω-plane on the m_1, m_2, m_3 planes, respectively. The following relations may be used to obtain the behavior for other ω:

$$m_1(-\omega) = -m_1(\omega);\ m_1(\bar{\omega}) = \bar{m}_1(\omega) \quad (22a)$$

$$m_2(-\omega) = m_2(\omega);\ m_2(\bar{\omega}) = \bar{m}_2(\omega) \quad (22b)$$

$$m_3(-\omega) = m_3(\omega);\ m_3(\bar{\omega}) = \bar{m}_3(\omega) \quad (22c)$$

where the bar denotes the complex conjugate.

For $|\omega| \gg \alpha^{1/2}$ and $|\arg\omega| < \pi/2$ the behavior is

$$m_1 \sim \kappa_1^{1/2}\omega\left\{1 - \frac{1}{2(1-\kappa_1)} \times \left[(\alpha+1) - \frac{1-\nu^2}{\kappa_1}\right]\omega^{-2} + 0[\omega^{-4}]\right\} \quad (23a)$$

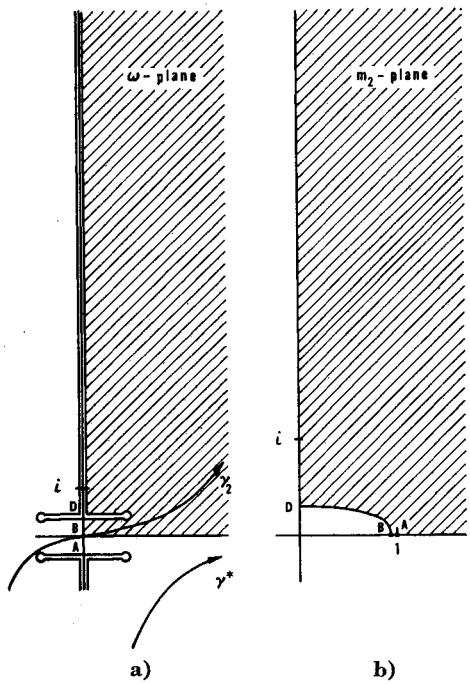

Fig. 5 Conformal mapping of the first quadrant of the ω-plane on the m_2-plane.

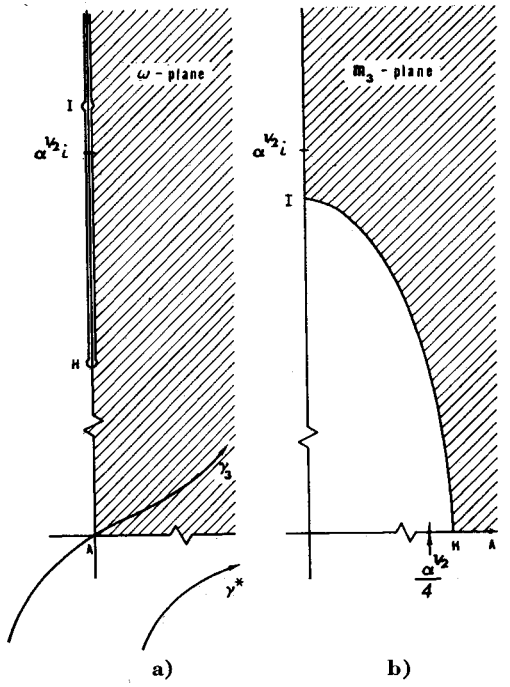

Fig. 6 Conformal mapping of the first quadrant of the ω-plane on the m_3-plane.

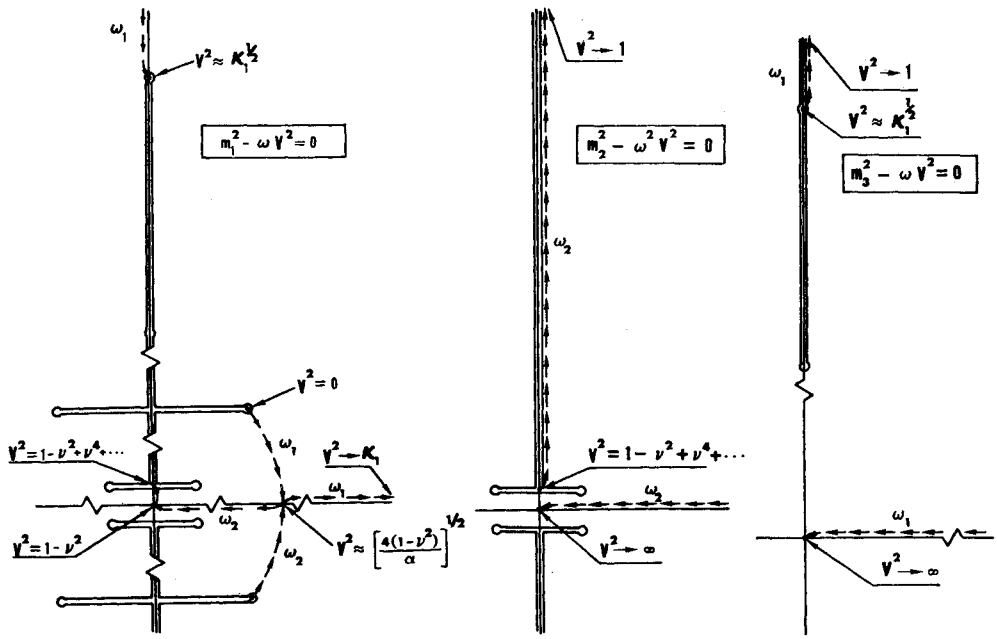

Fig. 7 Loci of poles in the ω-plane.

$$m_2 \sim \omega\{1 + 0[\omega^{-4}]\} \tag{23b}$$

$$m_3 \sim \omega\left\{1 + \frac{1}{2(1-\kappa_1)}[(\alpha+1) - (1-\nu^2)]\omega^{-2} + 0[\omega^{-4}]\right\} \tag{23c}$$

Respectively, the relations

$$m_1 \sim (1-\nu^2)^{1/2}\omega\{1 - (\nu^2/2)\omega^2 + 0[\omega^4]\} \tag{24a}$$

$$m_2 \sim 1 + \tfrac{1}{2}[\nu^2/2 - \kappa_1/(\alpha-1)]\omega^2 + 0[\omega^4] \tag{24b}$$

$$m_3 \sim \alpha^{1/2} + \tfrac{1}{2}[(1+\kappa_1) + \kappa_1/(\alpha-1)] \times \alpha^{-1/2}\omega^2 + 0[\omega^4] \tag{24c}$$

describe the behavior $m(\omega)$ for values $|\omega| \ll \alpha^{-1/2}$ and $|\arg\ \omega| < \pi/2$. To perform the integration indicated in Eq. (13), it is necessary to determine the loci of poles of the functions $\mathbf{b}_k(\omega)$, $\mathbf{b}_v(\omega)$, $\mathbf{b}_0(\omega)$ given in Eq. (14). The integral

$$\boldsymbol{\varepsilon}_0 = \frac{2}{\pi}\int_0^\infty \mathbf{b}_0 \sin(\omega\xi)d\omega \tag{25}$$

represents the solution for a semi-infinite cylindrical shell loaded by a uniform static pressure. The function $\mathbf{b}_0(\omega)$ has poles at the zeros of

$$m_1^2 m_2^2 m_3^2 = 0$$

which are $\omega = 0$; b_{11}; $-\bar{b}_{11}$; $-\bar{b}_{11}$; $-\bar{b}_{11}$. The contribution resulting from $\mathbf{b}_0$ is easily found by residue theory to be

$$\boldsymbol{\varepsilon}_{(0)} = \frac{1}{1-\nu^2}\begin{bmatrix}-\nu\\1\\0\end{bmatrix} + \Re e\left\{\left(-\frac{1}{1-\nu^2}\begin{bmatrix}-\nu\\1\\0\end{bmatrix} + \frac{1}{\kappa_1(b_{11}^{-2}-b_{11}^2)}\begin{bmatrix}-\nu\\1\\2\alpha\end{bmatrix}\right)e^{ib11\xi}\right\} \tag{26}$$

The denominator of $\mathbf{b}_v(\omega)$ is a polynomial of ω

$$\omega^{-1}[(\omega v)^2 - m_1^2][(\omega v)^2 - m_2^2][(\omega v)^2 - m_3^2] = \omega\{(v^2-1)^2(v^2-\kappa_1)\omega^4 - (v^2-1)[(\alpha+1)v^2 - (1-\nu^2)]\omega^2 + \alpha[v^2-(1-\nu^2)]\} = (v^2-1)^2(v^2-\kappa_1)\omega(\omega-\omega_1)(\omega+\omega_1)(\omega-\omega_2)(\omega+\omega_2)$$

and has the roots ω_1; $-\omega_1$; ω_2; $-\omega_2$ and $\omega_0 = 0$. Their loci are indicated for different load velocities in Fig. 7. Both of the roots ω_1 and ω_2 are, for small values of v^2, zeros of $(\omega v)^2 - m_1^2$. They are at $\omega_1 = b_{11}$ for $v^2 = 0$, then become real for v equal to the minimum phase velocity given in Eq. (17). For $v = (m/\omega)_{\min}$, $\mathbf{b}_v$ has two second-order poles located at $\omega_1(=\omega_2)$ and $-\omega_1$. With increasing load velocity v, ω_1 is shifted to higher real values and $\omega_1 \to \infty$ as $v^2 \to \kappa_1$, the "shear" velocity. For $v^2 > \kappa_1$, ω_1 is on the positive imaginary axis. At $v^2 \sim \kappa_1^{1/2}$, ω_1 passes through the branchpoint b_{31} (denoted by I in Fig. 7) to become a zero of $(\omega v)^2 - m_3^2$. With further increasing v, $\omega_1 \to \infty$ as $v^2 \to 1$, the "plate" velocity and jumps back to the real axis for values $v^2 > 1$. Finally, $\omega_1 \to 0$ as $v \to \infty$. The zero $\omega_2 \to 0$ as $v^2 \to (1-\nu^2)$. For $v^2 = (1-\nu^2)$, $\mathbf{b}_v$ has a third-order pole at $\omega = 0$. For $v^2 > 1-\nu^2$, ω_2 becomes positive imaginary. At $v^2 \sim 1 - \nu^2 + \nu^4 \ldots$, ω_2 crosses the branch cut (denoted by *BID* in Fig. 7) to become a zero of $(\omega\nu)^2 - m_2^2$. Then $\omega_2 \to i\infty$ as $v^2 \to 1$, and jumps back to the real axis for $v^2 > 1$. Finally, $\omega_2 \to 0$ as $v^2 \to \infty$.

The inversion integral Eq. (13) may be extended over the entire real axis

$$\boldsymbol{\varepsilon} = \frac{1}{\pi}\int_{-\infty}^{+\infty} \boldsymbol{\varepsilon}^{(s)} \sin(\omega\xi)d\omega \tag{27}$$

because $\boldsymbol{\varepsilon}^{(s)}(-\omega) = -\boldsymbol{\varepsilon}^{(s)}(\omega)$.

Since the poles of $\mathbf{b}_1$, $\mathbf{b}_2$, $\mathbf{b}_3$, $\mathbf{b}_v$, $\mathbf{b}_0$ cancel another, the integration path is shifted from the real axis to a contour γ_1 as indicated in Fig. 4a. If the integrand of Eq. (27) is written in exponential form, the contribution resulting from the terms with $\mathbf{b}_v$, $\mathbf{b}_0$ can be evaluated directly with aid of Jordan's Lemma and the Cauchy theorem. Using the fact

$$\int_{\gamma_1} \mathbf{b}_k e^{\pm i(m_k\tau+\omega\xi)}\,d\omega = -\int_{\bar{\gamma}_1} b_k e^{\pm i(m_k\tau-\omega\xi)}d\omega, \qquad k = 2,3$$

where $m_k(\omega)$ is an even function of ω and $\bar{\gamma}_1$ the contour conjugate to γ_1, and the relation

$$\int_{\gamma_1} f(\omega)e^{ig(\omega)}d\omega - \int_{\bar{\gamma}_1} f(\omega)e^{-ig(\omega)}d\omega = 2i\,\mathfrak{Im}\int_{\gamma_1} f(\omega)e^{ig(\omega)}d\omega$$

wherein $f(\omega)$, $g(\omega)$ have the behavior $f(\bar{\omega}) = \bar{f}(\omega), g(\omega) = \bar{g}(\omega)$, the inversion integral Eq. (27) is reduced to the form

$$\boldsymbol{\varepsilon} = \mathbf{R} - (1/2\pi)\mathfrak{Im}\left\{\int_{\gamma_1} \mathbf{b}_1 e^{-i(m_k\tau+\omega\xi)}d\omega + \int_{\bar{\gamma}_1} \mathbf{b}_1 e^{i(m_k\tau-\omega\xi)}d\omega\right\} - (1/\pi)\mathfrak{Im}\sum_{2,3}\int_{\gamma_k} \mathbf{b}_k e^{i(m_k\tau-\omega\xi)}d\omega \tag{28}$$

where γ_k the integration contour as indicated in Figs. 4a, 5a, and 6a.

For points behind the load front ($v\tau > \xi$), $\mathbf{R}$ has the form

$$\mathbf{R}(v\tau > \xi) = \begin{cases} \boldsymbol{\varepsilon}_0 & \text{for } v^2 < \kappa_1 \text{ and } v^2 > 1 \quad (29a) \\ \boldsymbol{\varepsilon}_0 + \mathbf{r}_1[e^{-|\omega_1|(v\tau+\xi)} - e^{-|\omega_1|(v\tau-\xi)}] & \\ \qquad \text{for } \kappa_1 < v^2 < 1 - \nu^2 + \nu^4 \ldots \quad (29b) \\ \boldsymbol{\varepsilon}_0 + \mathbf{r}_1[e^{-|\omega_1|(v\tau+\xi)} - e^{-|\omega_1|(v\tau-\xi)}] + & \\ \mathbf{r}_2[e^{-|\omega_2|(v\tau+\xi)} - e^{-|\omega_2|(v\tau-\xi)}] & \\ \qquad \text{for } 1 - \nu^2 + \nu^4 \ldots < v^2 < 1 \quad (29c) \end{cases}$$

and for points in front of the load discontinuity

$$\mathbf{R}(v\tau < \xi) = \mathbf{R}(v\tau > \xi) + \mathbf{r}_1[e^{i\omega_1(v\tau-\xi)} + e^{-i\omega_1(v\tau-\xi)} - e^{i\omega_2(v\tau-\xi)} - e^{-i\omega_2(v\tau-\xi)}] + \frac{1}{v^2 - (1-\nu^2)}\begin{bmatrix} -\nu \\ 1 - v^2 \\ 0 \end{bmatrix} \times \left\{1 - \frac{1}{2}[e^{i\omega_2(v\tau-\xi)} + e^{-i\omega_2(v\tau-\xi)}]\right\} \quad (30)$$

where $\boldsymbol{\varepsilon}_0$ is given in Eq. (26). The expressions $\mathbf{r}_1$, $\mathbf{r}_2$ are the residues of $\mathbf{b}_v$ at $\omega = \omega_1, \omega_2$, respectively

$$\mathbf{r}_1 = \lim_{\omega \to \omega \pm \omega_1} (\omega \mp \omega_1)\mathbf{b}_v = \begin{cases} -\lim_{\omega \to \pm\omega_1} (\omega \mp \omega_1)\mathbf{b}_1 & \text{for } v^2 < \kappa_1^{1/2} + \ldots \\ -\lim_{\omega \to \pm -\omega_1} (\omega \mp \omega_1)\mathbf{b}_3 & \text{for } v^2 > \kappa_1^{1/2} + \ldots \end{cases} =$$

$$\frac{1}{(v^2-1)^2(v^2-\kappa_1)\omega_1^2(\omega_1^2-\omega_2^2)}\begin{bmatrix} -\nu[\alpha + \omega_1^2(1-v^2)] \\ (1-v^2)[\alpha + \omega_1^2(1-v^2)] \\ \alpha\omega_1^2(1-v^2) \end{bmatrix} \quad (31)$$

and

$$\mathbf{r}_2 = \lim_{\omega \to \pm\omega_2} (\omega \mp \omega_2)\mathbf{b}_v = \begin{cases} -\lim_{\omega \to \pm\omega_2} (\omega \mp \omega_2)\mathbf{b}_1 & \text{for } v^2 < 1 - \nu^2 + \nu^4 \ldots \\ -\lim_{\omega \to \pm\omega_2} (\omega \mp \omega_2)\mathbf{b}_2 & \text{for } v^2 > 1 - \nu^2 + \nu^4 \ldots \end{cases} = -\frac{1}{2[v^2 - (1-\nu^2)]}\begin{bmatrix} -\nu \\ 1 - v^2 \\ 0 \end{bmatrix} - \mathbf{r}_1 \quad (32)$$

For points on the shell ahead of the "plate" velocity front ($\xi > \tau$) the integrals in Eq. (28) can be evaluated exactly by shifting the integration contour to the lower half circle of the ω-plane and using Jordan's Lemma;

$$\boldsymbol{\varepsilon} = \mathbf{R}^* = \begin{cases} 0 & \text{for } \xi > v\tau \\ -\frac{1}{v^2 - (1-\nu^2)}\begin{bmatrix} -\nu \\ 1 - v^2 \\ 0 \end{bmatrix} \times & \\ \{1 - \cos\omega_2(v\tau - \xi)\} - 2\mathbf{r}_1[\cos\omega_1(v\tau - \xi) - & \\ \cos\omega_2(v\tau - \xi)] \qquad \text{for } v\tau > \xi \quad (33 \end{cases}$$

Asymptotic Evaluation

The integrals given in Eq. (28) cannot be evaluated in closed form, except for points ahead of the plate velocity $\xi/\tau > 1$ where the three integrals vanish. In the following, an asymptotic representation as $\tau \to \infty$ will be obtained using methods discussed by Felsen and Marcuvitz[9] and utilized for the beam with a moving load in Refs.[3,4] First, the integrand is given a partial-fraction decomposition for each pole on the real axis

$$\mathbf{b}_1 = \mathbf{r}_0(1/\omega) + \begin{cases} \mathbf{R}_{11} & \text{for } v^2 < (m/\omega)_{\min} \text{ and } v^2 > 1 - \nu \\ -\mathbf{r}_1[1/(\omega - \omega_1) + 1/(\omega + \omega_1)] - & \\ \mathbf{r}_2[1/(\omega - \omega_2) + 1/(\omega + \omega_2)] + \mathbf{R}_{12} & \\ \qquad \text{for } (m/\omega)_{\min} < v^2 < \kappa_1 & \\ -\mathbf{r}_2[1/(\omega - \omega_2) + 1/(\omega + \omega_2)] + \mathbf{R}_{13} & \\ \qquad \text{for } \kappa_1 < v^2 < 1 - \nu^2 \quad (34a) \end{cases}$$

$$\mathbf{b}_2 = \begin{cases} \mathbf{R}_{21} & \text{for } v^2 < 1 \\ -\mathbf{r}_2[1/\omega - \omega_2 + 1/\omega + \omega_2] + \mathbf{R}_{22} & \\ \qquad \text{for } v^2 > 1 \quad (34b) \end{cases}$$

$$b_3 = \begin{cases} \mathbf{R}_{31} & \text{for } v^2 < 1 \\ -\mathbf{r}_1[1/(\omega - \omega_1) + 1/(\omega + \omega_1)] + \mathbf{R}_{31} & \\ \qquad \text{for } v^2 > 1 \quad (34c) \end{cases}$$

where

$$\mathbf{r}_0 = \lim_{\omega \to 0} \omega\, \mathbf{b}_1 = \frac{\nu^2}{(1-\nu^2)[v^2 - (1-\nu^2)]}\begin{bmatrix} -\nu \\ \nu^2 \\ 0 \end{bmatrix} \quad (35)$$

and $\mathbf{r}_1$,$\mathbf{r}_2$ are given by Eqs. (31) and (32). Then, the remainder terms $\mathbf{R}_{ik}$ are analytic on the real axis and their integrals may be easily evaluated by the method of stationary phase.[7,8]

Since the saddlepoints of the integrand

$$e^{-i(m_1\tau + \omega\xi)}\omega - \omega_0$$

are always far away from the pole on the real axis in the lower ω-half-plane, the contour γ_1 is shifted to the path of steepest descent without passing the pole. Its integral is

$$\int_{\gamma_1}[e^{-i(m_1\tau+\omega\xi)}d\omega/(\omega - \omega_0)] \sim 0(\tau^{-1/2}) \quad (36)$$

For very thin shells ($h/a \ll 0.02)(\partial m_1/\partial\omega)_{\min}$ can be smaller than zero. Then the integrand has two saddlepoints on the real axis when $\xi/\tau < [(\partial m_1/\partial\omega)_{\min}]$ and the asymptotic behavior may be evaluated in an analogous way as given for the integral type $e^{i(m_1\tau-\omega\xi)}$. The integrands $e^{i(m_{2,3}\tau-\omega\xi)}d\omega/(\omega - \omega_0)$ have one saddlepoint ω_s on the real positive axis, given by $(\partial m_{2,3}/\partial\omega - \xi/\tau)\omega_s = 0$. So the integral is transformed to the saddlepoint variable u where

$$u(\omega) = [(m_{2,3}\tau - \omega\xi) - (m_{2,3}\tau - \omega\xi)\omega_s]^{1/2} = \left[\frac{\tau}{2}\left(\frac{\partial^2 m_{2,3}}{\partial\omega^2}\right)_{\omega_s}\right]^{1/2}(\omega - \omega_s) + 0[(\omega + \omega_s)^2] \quad (37)$$

$$\int \frac{e^{i(m_{2,3}\tau-\omega\xi)}d\omega}{\omega - \omega_0} = \int \frac{e^{iu^2}}{u - u(\omega_0)}\, g(u)du$$

where

$$g(u) = \{[u - u(\omega_0)]/(\omega - \omega_0)\}d\omega/du$$

When the pole ω_0 is far away from the saddlepoint $g(u)/[u - u(\omega_0)]$ is regular near $u = 0$ and can be expanded into a power series

$$[g(u)/u - u(\omega_0)] = [g(u)/\{u - u(\omega_0)\}]_{u=0} + [g(u)/\{u - u(\omega_0)\}]'_{u=0}\, u + \ldots$$

Thus, the first-order term of the asymptotic expansion is

$$\int [e^{i(m_{2,3}\tau-\omega\xi)}d\omega/(\omega - \omega_0)] \sim 0(\tau^{-1/2}) \quad (38)$$

When ω_0 is close to ω_s, $g(u)$ is regular in the vicinity $u = 0$, and can be expanded into a power series

$$g(u) = g(u_0) + g'(u_0)(u - u_0) + \ldots$$

and the asymptotic behavior is represented by

$$\int_{\gamma_{2,3}} [e^{i(m_{2,3}\tau-\omega\xi)}d\omega/(\omega - \omega_0)] \sim 2\pi i e^{i\omega_0(v\tau-\xi)} I[u(\omega_0)] \quad (39)$$

where $\gamma_{2,3}$ is a contour passing below the pole at ω_0 and $I[u(\omega_0)]$, is the error function as utilized in Ref. 5

$$I[u(\omega_0)] = \pi^{-1/2} e^{i(\pi/4)} \int_{-\infty}^{u(\pi_0)} e^{-iu^2} du$$

The integrand $e^{i(m_1\tau-\omega)}/(\omega - \omega_0)$ has 1) two separated first-order saddlepoints in the upper ω-half plane when $\xi/\tau < (\partial m_1/\partial\omega)_{\min}$; 2) two separated first-order saddlepoints on the real axis and two neighboring saddlepoints near the origin when $(\partial m_1/\partial\omega)_{\min} < \xi/\tau < \kappa_1^{1/2}$; 3) two neighboring saddlepoints near the origin when $\xi/\tau > \kappa_1^{1/2}$. The integration along the paths indicated in Fig. 8 is performed by considering the contribution to the integral from the portion of the contour near the saddlepoints. The solid lines denote the paths of steepest descent. The evaluation of the asymptotic behavior for case 1 is analogous to that given in Eq. (36), because the saddlepoints are far away from the pole on the real axis. The contribution to the integral resulting from the two separated saddlepoints in case 2 can be obtained using Eqs. (38) and (39).

The steepest descent procedure utilized to evaluate the integrals with a separated saddlepoint is no longer applicable when two saddlepoints are sufficiently close to one another, case 2 and 3. Then the integral is transformed to an Airy function type of integral whose integrand also contains two saddlepoints

$$\int \frac{e^{i(m_1\tau-\omega\xi)}d\omega}{\omega - \omega_0} = \int \frac{e^{i(xt-t^3/3)}}{\tau - \tau(\omega_0)} g(t)\, dt \qquad (40)$$

where

$$g(t) = [t - t(\omega_0)]/\omega - \omega_0]d\omega/dt$$

and

$$x = [\tfrac{3}{2}(m_1 - \omega\xi/\tau)_{\omega_s}]^{2/3}\tau^{2/3} \qquad (41)$$

In the region of interest $(\partial m_1/\partial\omega)_{\min} < \xi/\tau < 1$, x is real and

$$x > 0 \text{ when } (\partial m/\partial\omega)_{\min} < \xi/\tau < (1 - \nu^2)^{1/2}$$

$$x < 0 \text{ when } \xi/\tau > (1 - \nu^2)^{1/2}$$

When the pole ω_0 is not close to the origin $\omega = t = 0$, $[g(t)/t - t(\omega_0)]$ is regular near $t = 0$ and can be expanded into a power series and the first-order approximation gives

$$\int_\Gamma \frac{e^{i(m_1\tau-\omega\xi)}d\omega}{\omega - \omega_0} \sim 2\pi i \left[\frac{g(t)}{t - t(\omega_0)}\right]_{t=0} Ai[-x] = 0(\tau^{-1/3}) \qquad (42)$$

When the pole ω_o is near $\omega = 0$, $g(t)$ is regular near $\omega = \omega_0$ and can be expanded into a power series

$$g(t) = g[t(\omega_0)] + g'[t(\omega_0)][t - t(\omega_0)] + \ldots$$

Introducing the power series expansion into Eq. (40) the integral has the first-order term approximation

$$\int_\Gamma [e^{i(m_1\tau-\omega\xi)}d\omega/(\omega - \omega_0)] \sim g[t(\omega_0)]G_{(1)}[x,t(\omega_0)] \qquad (43)$$

where the evaluation of $G_{(1)}[x,t(\omega_o)]$ is performed in the Appendix. Γ is a contour passing below the pole at ω_0. When $\omega_0 = t[\omega_0] = 0\, g[t(\omega_0)] = g(0) = 1$.

With the aid of Eqs. (36, 38, 39, 42, 43) the contribution of each integral term to $\boldsymbol{\varepsilon}$ is evaluated and a first-order term approximation can be obtained. Introducing the following abbreviations

$$\mathbf{A}(\omega_k) = 0 \qquad \text{for } \omega_{s_{12}} < \omega_k$$

$$\mathbf{A}(\omega_k) = \Re\mathbf{e}\mathbf{r}_k \times \begin{cases} [e^{i\omega_k(v\tau-\xi)} + e^{-i\omega_k(v\tau-\xi)}][1 - I[u(\omega_k)] & \text{for } \omega_{s_{12}} = 0(\omega_k) \\ [e^{i\omega_k(v\tau-\xi)} + e^{-i\omega_k(v\tau-\xi)}] & \text{for } \omega_{s_{12}} < \omega_k \end{cases} \qquad (44)$$

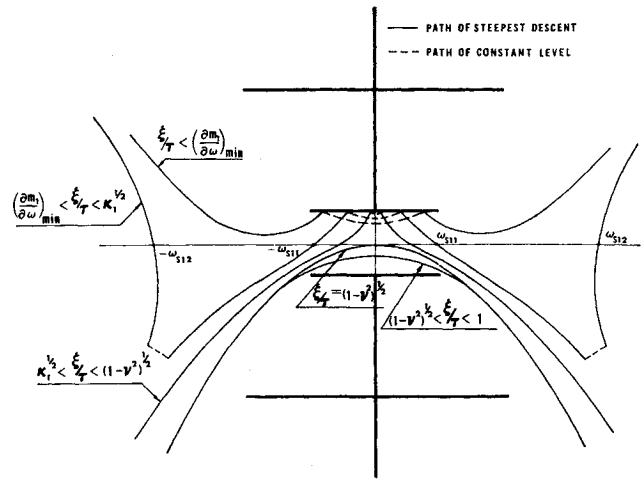

Fig. 8 Integration contour lines for different ξ/τ.

where $u(\omega_k) = [\omega_k(v\tau - \xi) - (m_1\tau - \omega\xi)\omega_{s_{12}}]^{1/2}$, $\mathbf{r}_k$ is given in Eqs. (31) and (3)

$$\mathbf{B}(\omega_{sj},\omega_k) = -2\Re\mathbf{e}\mathbf{r}_k \times \begin{cases} e^{i\omega_k(v\tau-\xi)} & \text{for } \omega_{s_j} < \omega_k \\ e^{i\omega_k(v\tau-\xi)}I[u(\omega_{sj}\omega_k)] & \text{for } \omega_{s_j} = 0(\omega_k) \\ 0 & \text{for } \omega_{s_j} > \omega_k \end{cases} \qquad (45)$$

where $u(\omega_{sj},\omega) = [\omega_k(v\tau - \xi) - (m_j\tau - \omega\xi)\omega_{sj}]^{1/2}$ $j = 2,3$ and

$$\mathbf{D}(x) = \frac{v^2}{(1 - \nu^2)[v^2 - (1 - \nu^2)]} \begin{bmatrix} -\nu \\ 1 \\ 0 \end{bmatrix} [1 - G_{(1)}(x)] \qquad (46)$$

the solution is

$$\boldsymbol{\epsilon} = \begin{cases} \mathbf{R}(v\tau > \xi) + 0(\tau^{-1/2}) & \text{for } \xi/\tau < v \\ \mathbf{R}(v\tau < \xi) + 0(\tau^{-1/2}) & \text{for } v < \xi/\tau^2(\partial m_1/\partial\omega)_{\min} \\ \mathbf{R}(v\tau < \xi) + \mathbf{D}(x) + 0(\tau^{-1/3}) & \\ & \text{for } \xi/\tau > (\partial m_1/\partial\omega)_{\min} \end{cases} \qquad (47)$$

when $v^2 < (m_1/\omega)^2_{\min}$ $\mathbf{R}(v\tau > \xi)$,$\mathbf{R}(v\tau < \xi)$ and x are given in Eqs. (29), (30) and (42), respectively. Aside from the last term $\mathbf{D}(x)$, the solution is identical with that found for the Timoshenko beam on elastic foundation.[4] Since the coefficient of $\mathbf{D}(x)$

$$\{v^2/(1 - \nu^2)[v^2 - (1 - \nu^2)]\} < [4(1 - \nu^2)\kappa_1/\alpha]^{1/2} \ll 1$$

the influence of that term on $\boldsymbol{\varepsilon}$ is negligible in comparison with $\mathbf{R}(v\tau < \xi)$ which is 0(1). When $(m/\omega)_{\min} < v^2 < \kappa_1$ the poles at $\omega = \pm\omega_2$—as indicated in Fig. 9a—are still far away from the origin. Thus the solution is

$$\boldsymbol{\varepsilon} = \begin{cases} \mathbf{R}(v\tau > \xi) + 0(\tau^{-1/3}) & \text{for } \xi/\tau < (\partial m_1/\partial\omega)_{\min} \quad (48a) \\ \mathbf{R}(v\tau > \xi) + \mathbf{A}(\omega_1) + \mathbf{A}(\omega_2) + \mathbf{D}(x) + 0(\tau^{-1/3}) & \\ & \text{for } (\partial m_1/\partial\omega)_{\min} < \xi/\tau < v \quad (48b) \\ \mathbf{R}(v\tau < \xi) + \mathbf{A}(\omega_1) + \mathbf{A}(\omega_2) + \mathbf{D}(x) + 0(\tau^{-1/3}) & \\ & \text{for } \xi/\tau > v \quad (48c) \end{cases}$$

Since $\mathbf{D}(x)$ is still small in comparison with $\mathbf{R}(v\tau > \xi)$, $\mathbf{R}(v\tau < \xi)$ the solution for the Timoshenko beam would be a useful approximation for the cylindrical shell.

For load velocities $\kappa_1 < v^2 < 1 - \nu^2$ the poles on the real axis are at $\omega = 0, \pm\omega_2$. As the velocity increases, ω_2 becomes a

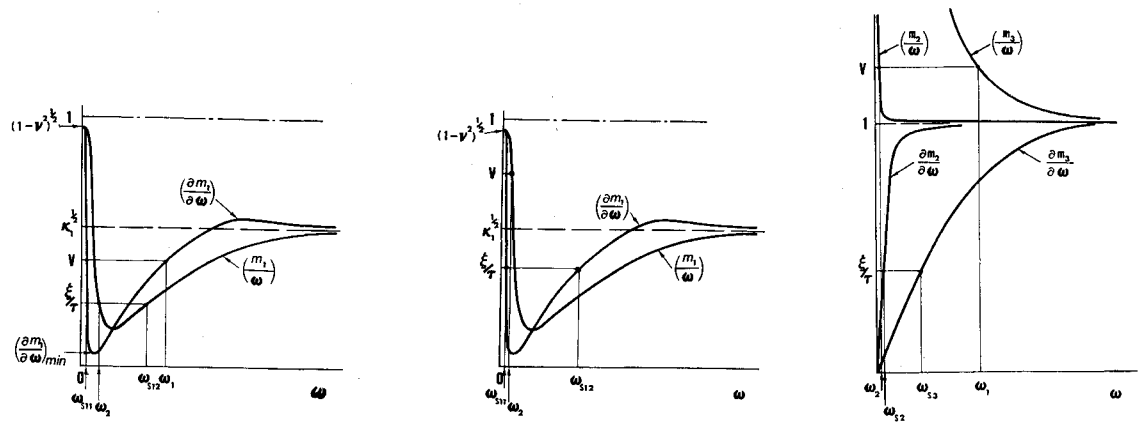

Fig. 9 Loci of saddlepoints and poles for different load velocities.

pole near the origin (Fig. 9b). Thus the solution is

$$\epsilon = \begin{cases} \mathbf{R}(v\tau > \xi) + 0(\tau^{-1/2}) & \text{for } \xi/\tau < (\partial m/\partial\omega)_{\min} \\ \mathbf{R}(v\tau > \xi) + \mathbf{C}(\omega_2) + \mathbf{D}(x) + 0(\tau^{-1/3}) & \\ \qquad \text{for } (\partial m/\partial\omega)_{\min} < \xi/\tau < v & \\ \mathbf{R}(v\tau < \xi) + \mathbf{C}(\omega_2) + \mathbf{D}(x) + 0(\tau^{-1/3}) & \\ \qquad \text{for } \xi/\tau > v & (49) \end{cases}$$

where

$$\mathbf{C}(\omega_2) = \Re e\ \mathbf{r}_2 \{e^{i\omega_2(v\tau-\xi)} - G_{(1)}[x,t(\omega_2)] + e^{-i\omega_2(v\tau-\xi)} - G_{(1)}[x,t(-\omega_2)]\}$$

with

$$t(\pm\omega_2) \sim \pm\omega_2 \frac{(1-\nu^2)^{1/2} - \xi/\tau}{[\frac{3}{2}(m_1 - \xi/\tau)\omega_{s_{11}}]^{2/3}} \tau^{1/3}$$

and $G_{(1)}[x,t(\omega_0)]$ as defined in the Appendix. The term $\mathbf{D}(x)$ which is characteristic for the cylindrical shell becomes the dominant part of the solution as v approaches the "bar" velocity, $v^2 \to (1-\nu^2)$. For $(1-\nu^2) < v^2 < 1$ the only pole on the real axis is at $\omega = 0$, so the solution is

$$\epsilon = \begin{cases} \mathbf{R}(v\tau > \xi) + 0(\tau^{-1/3}) & \text{for } \xi/\tau < (\partial m_1/\partial\omega)_{\min} \\ \mathbf{R}(v\tau > \xi) + \mathbf{D}(x) + 0(\tau^{-1/3}) & \\ \qquad \text{for } (\partial m_1/\partial\omega)_{\min} < \xi/\tau < v & (50) \\ \mathbf{R}(v\tau < \xi) + \mathbf{D}(x) + 0(\tau^{-1/3}) \text{ for } \xi/\tau > v & \end{cases}$$

For $v_2 > 1$ the poles at $\pm\omega_1$, $\pm\omega_2$ are again on the real axis, and the solution is

$$\epsilon = \begin{cases} \mathbf{R}(v\tau > \xi) + \mathbf{B}(\omega_{s_2},\omega_2) + \mathbf{B}(\omega_{s_2},\omega_1) + 0(\tau^{-1/3}) & \\ \qquad \text{for } \xi/\tau < (\partial m_1/\partial\omega)_{\min} & \\ \mathbf{R}(v\tau > \xi) + \mathbf{B}(\omega_{s_2},\omega_2) + \mathbf{B}(\omega_{s_2},\omega_1) + \mathbf{D}(x) + 0(\tau^{-1/3}) & \\ \qquad \text{for } \partial m_1/\partial\omega_{\min} < \xi/\tau < 1 & \\ \mathbf{R}^* \qquad \text{for } \xi/\tau > 1 & (51) \end{cases}$$

where $\mathbf{R}^*$ is given in Eq. (33).

The boundary velocity between the different regions of load velocities, whose solutions are given in Eqs. (47–51), are the so-called critical velocities for which the steady-state solution[1,2] gives an unbounded response of the shell.

The velocities are

1) $v = \left(\frac{m_1}{\omega}\right)_{\min} \sim \left[\frac{4(1-\nu^2)\kappa_1}{\alpha}\right]^{1/4} \times$ minimum phase velocity)

2) $v = \kappa^{1/2}$ (shear velocity)

3) $v = (1-\nu^2)^{1/2}$ (bar velocity)

4) $v = 1$ (plate velocity)

For case 1, when v is equal to the minimum phase velocity, the inversion integral has two second-order poles at $\omega = \pm\omega_1$, $\pm\omega_2$, which are on the real axis

$$\omega_1 \sim \{[(1-\nu^2)/\kappa_1]\alpha\}^{1/4}$$

and zeros of $m_1^2 - (\omega_1 v)^2 = 0$. The solution is

$$\epsilon = -\frac{1}{2\tau} \Im m \mathbf{r}_{1_2} \int_{\gamma_1} \left\{\frac{1}{(\omega-\omega_1)^2} - \frac{1}{(\omega+\omega_1)^2}\right\} \times e^{i(m_1\tau+\omega\xi)} d\omega + 0(1) \quad (52)$$

where

$$r_{1_2} = \frac{1}{4\omega_1^3(1-v^2)(\kappa_1-v^2)} \begin{bmatrix} -v[(1-v^2)\omega_1^2 + \alpha] \\ (1-v^2)[(1-v^2)\omega_1^2 + \alpha] \\ \alpha(1-v^2)\omega_1^2 \end{bmatrix} \sim \frac{1}{4}\left[\frac{\alpha}{(1-\nu^2)^3\kappa_1}\right]^{1/4} \begin{bmatrix} -\nu \\ 1 \\ \left(\frac{1-\nu^2}{\kappa_1}\alpha\right)^{1/2} \end{bmatrix}$$

Since these poles are far away from the neighboring two saddlepoints near the origin, the asymptotic representation of the inversion integral can be obtained in a way similar to that given in Ref. 4 for the Timoshenko beam. The result is the behavior $\epsilon \sim 0(\tau^{1/2})$ for points near the load front. Thus ϵ increases with the square root of the distance of the load front from the end of the shell. Therefore, $v = (m_1/\omega)_{\min}$ is a "critical" velocity, in that it can cause a large amplitude of response in a long shell.

For cases II and IV, for load velocities equal to the shear velocity $v = \kappa_1^{1/2}$ or the "plate" velocity $v = 1$, the inversion integral has simple poles at infinity. As indicated in Ref. 4 the solution ϵ remains $0(1)$ as v reaches these velocities. Since the solution is bounded $v = \kappa_1^{1/2}$ and $v = 1$ are not actually critical velocities, even though a steady-state solution does not exist.

For case III, when the load velocity v is equal to the bar velocity $v = (1-\nu^2)^{1/2}$, the integrand of the inversion integral has a third pole at zero and two simple poles on the imaginary axis at

$$\omega = \pm\omega_1, \text{ where } \omega_1 = i[\alpha(1-\nu^2)/(1-\nu^2-\kappa_1)\nu^2]^{1/2}$$

As described in the preceding section, the integration contour is shifted to a contour γ_1 passing below the pole at zero. Then

$$\epsilon = \mathbf{R}_{(1-\nu^2)} - (1/2\pi)\Im m\{\textstyle\int_{\bar\gamma_1} \mathbf{b}_1 e^{i(m_1\tau-\omega\xi)}\, d\omega + \int_{\gamma_1} \mathbf{b}_1 e^{i(m_1\tau-\xi)} d\omega\} - (1/\pi)\Im m \int_{\gamma_1} \sum_{2,3} \mathbf{b}_k e^{i(m_k\tau-\omega\xi)} d\omega$$

where

$$\mathbf{R}(1-\nu^2)=\begin{cases}\varepsilon_0-\dfrac{1}{2\alpha(1-\nu^2)^2}\begin{bmatrix}-\kappa_1\nu\\ \kappa_1\nu^2\\ \alpha(1-\nu^2)\end{bmatrix}[e^{i\omega_1(v\tau+\xi)}+e^{i\omega_1(v\tau-\xi)}]+\begin{bmatrix}0\\1\\0\end{bmatrix}\cos\tau & \text{for } \xi/\tau<v\\ \varepsilon_0+\dfrac{1}{2\alpha(1-\nu^2)^2}\begin{bmatrix}-\kappa_1\nu\\ \kappa_1\nu^2\\ \alpha(1-\nu^2)\end{bmatrix}[2-e^{i\omega_i(v\tau+\xi)}-e^{-i\omega_1(v\tau-\xi)}]+\begin{bmatrix}0\\1\\0\end{bmatrix}\cos\tau-\frac{1}{2}\times & \\ \qquad\begin{bmatrix}-\dfrac{1}{\nu}\\ 1\\ 0\end{bmatrix}(v\tau-\xi)^2 & \text{for } \xi/\tau>v\end{cases} \tag{53}$$

and $\mathbf{b}_1$, $\mathbf{b}_2$ are given a partial-fraction decomposition for the poles at zero

$$\mathbf{b}_1=-\frac{1}{1-\nu^2}\begin{bmatrix}-\dfrac{1}{\nu}\\ 1\\ 0\end{bmatrix}\frac{1}{\omega^3}-\left\{\frac{1}{\alpha(1-\nu^2)^2}\times\begin{bmatrix}-\kappa_1\nu\\ \alpha(1-\nu^2)^2+\nu^2\kappa_1\\ \alpha(1-\nu^2)\end{bmatrix}-\frac{1}{1-\nu^2}\begin{bmatrix}-\nu\\1\\0\end{bmatrix}\right\}\frac{1}{\omega}+\mathbf{R}_1$$

$$\mathbf{b}_2=\begin{bmatrix}0\\1\\0\end{bmatrix}\frac{1}{\omega}+\mathbf{R}_2 \tag{54}$$

Since $\mathbf{R}_1,\mathbf{R}_2,\mathbf{b}_3$ are regular on the real axis, their integrals can be evaluated as performed before. The third-order pole at zero lies between two neighboring saddlepoints when $\xi/\tau > (\partial m_1/\partial\omega)_{\min}$. Therefore, the integral is transformed to an Airy function type of integral

$$\int_\Gamma \frac{e^{i(m_1\tau-\omega\xi)}}{\omega^3}\,d\omega=\int_\Gamma\frac{e^{i(xt-t^3/3)}}{t^3}\,g(t)dt$$

with x as given in Eq. (41).
Since x is real in the region of interest, the function

$$g(t)=(t^3/\omega s)(d\omega/dt)$$

is regular near $\omega=t=0$ and can be expanded into a power series

$$g(t)=g(0)+g'(0)t+g''(0)t^2/2+\ldots$$

when $\omega^2\ll 1$, m_1 was the behavior

$$m_1=(1-\nu^2)^{1/2}\{\omega-(\nu^2/2)\omega^3+\ldots\}$$

$$(m_1\tau-\omega\xi)=[(1-\nu^2)^{1/2}-\xi/\tau]\tau\omega-(1-\nu^2)^{1/2}(\nu^2/2)\tau\omega^2+\ldots=xt-t^3/3$$

and

$$\omega=\alpha_1 t+\alpha_3 t^3+\alpha_5 t^5+\ldots$$

where

$$\alpha_1=\frac{\{\frac{3}{2}[m_1-(\xi/\tau)\omega]_{\omega s}\}^{2/3}}{(1-\nu^2)^{1/2}-\xi/\tau}\,\tau^{-1/3}$$

Then

$$g(0)=\alpha_1^{-2},\ g'(0)=g''(0)=g'''(0)=0$$

and

$$\int_\Gamma\frac{e^{i(m_1\tau-\omega\xi)}}{\omega^3}\,d\omega\sim\alpha_1^{-2}\int_\Gamma\frac{e^{i(xt-t^3/3)}}{t^3}\,dt+0(\tau^{-1/3})$$

The evaluation of

$$G_{(3)}(x)=\textstyle\int_\Gamma[e^{i(xt-t^3/3)}/t^3]\,dt$$

is performed in the Appendix. Then the asymptotic behavior of $\boldsymbol{\varepsilon}$ for $v^2=1-\nu^2$ is

$$\boldsymbol{\varepsilon}=\begin{cases}\mathbf{R}(1-\nu^2)+0(\tau^{-1/2}) & \text{for } \xi/\tau\ll v\\ \dfrac{[\frac{3}{2}\nu^2(1-\nu^2)]^{2/3}}{2(1-\nu^2)}\begin{bmatrix}-\dfrac{1}{\nu}\\1\\0\end{bmatrix}\tau^{2/3}\times\begin{cases}c_1+2c_2x-\frac{2}{3}x^2+\ldots\\ c_1+2c_2x+\frac{1}{3}x^2+\ldots\end{cases}+0(1) & \begin{matrix}\text{for } \xi/\tau\le v\\ \text{for } \xi/\tau\ge v\end{matrix}\\ 0 \qquad \text{for } \xi/\tau\ge 1\end{cases} \tag{55}$$

where

$$x=\{(1-\nu^2)^{1/2}-\xi/\tau/[\tfrac{3}{2}\nu^2(1-\nu^2)^{1/2}]^{1/3}\}\tau^{2/3}$$

Thus the solution increases with $\tau^{2/3}$ in the near vicinity of the load front. Since τ is proportional to the distance of the load front from the end of the shell, the amplitude of the strain vector $\boldsymbol{\varepsilon}$ near the load front can become large for long shells. So, $v^2=1-\nu^2$ is a critical velocity. The solution is well behaved away from the load discontinuity.

Closure

After coming through all the preceding mathematical manipulation, we see that the most interesting features, from the viewpoint of a design engineer, can be described rather simply. There are two critical speeds; one equal to the bar velocity $(E/\rho)^{1/2}$ and the other much lower $[3(1-\nu^2)]^{-1/4}(h/a)^{1/2}(E/\rho)^{1/2}$ (Fig. 10). For load speeds less than the lower critical velocity, the static solution is reasonably good; for load speeds greater than the bar velocity, the cylinder is, essentially instantaneously loaded so the maximum stresses are roughly twice those of the static solution. The dynamic amplification factor of about two also holds for speeds between the two critical speeds. At the lower critical speed the response increases with the distance the load travels along the cylinder, giving a dynamic amplification factor of about $0.3[x/(ah)^{1/2}]^{1/2}$. Thus, for shells whose length is much greater than the "edge zone" of the static bending solution, a load moving at or near the lower critical velocity can produce a response much larger than the static solution (Fig. 11).

For the load moving at the bar velocity, the dynamic amplification factor also increases with the distance and is about, for $\nu=0.3$, $0.17(x/a)^{2/3}$. This critical velocity will therefore be important only for cylinders whose length is large in comparison with the radius (Fig. 11).

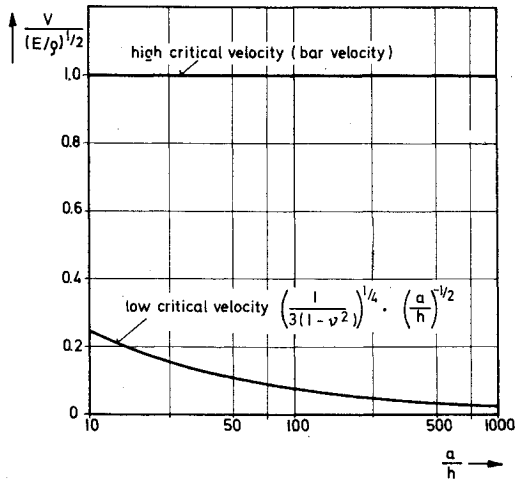

Fig. 10 Critical load velocities.

It may be of interest that, following the lines of the preliminary investigation given in Ref. 11 of load speeds which vary as the load moves along the shell, it appears that all four of the speeds at which no steady-state solution exists may be important. Caustics, which are region of stress intensification, form when the load accelerates through the minimum phase velocity and through the plate velocity. For a declerating load, however, caustics form when the load speed equals the "bar" and shear velocities. But, since the constant speed load moving at the shear or plate velocities does not cause particular trouble, one would expect the most severe stresses at the point where the load either accelerates through the minimum phase velocity, or decelerates through the bar velocity.

Appendix

Consider the integral

$$G_{(1)}(x,\omega_0) = \int_\Gamma [e^{i(x\omega-\omega^3/3)}/(\omega - \omega_0)]d\omega$$

where x, ω_0 are real constants and Γ is a contour from $-\infty$ to $+\infty$ passing below the pole at $\omega = \omega_0$. The integrand has two saddlepoints

$$(\partial/\partial\omega)(x\omega - \omega^3/3) = 0 \quad \text{at } \omega_s = \pm x^{1/2}$$

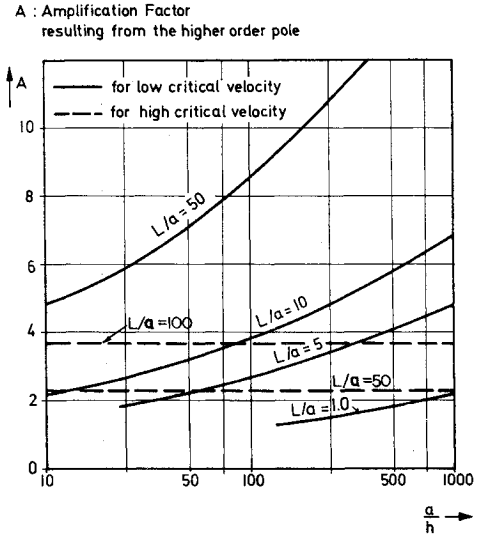

Fig. 11 Dynamic amplification factor for the critical load velocities.

Then

$$\frac{\partial(G_{(1)}e^{-ix\omega_0})}{\partial x} = i\int_\Gamma \exp\left\{i\left[x(\omega - \omega_0) - \frac{\omega^3}{3}\right]\right\}d\omega = 2\pi i\, e^{-ix\omega_0}Ai[-x]$$

and

$$G_{(1)}(x,\omega_o) = 2\pi i\, e^{ix\omega_0}\int_{-\infty}^{x} e^{-i\omega_0 s}Ai[-s]ds$$

where $Ai(x)$ denotes the Airy function.[10] For the special case $\omega_0 = 0$ integral $G_{(1)}(x,0)$ can be evaluated exactly

$$G_{(1)}(x) = 2\pi i\left\{\frac{1}{3} + \int_0^x Ai[-s]ds\right\}$$

From Ref. 10, $G_{(1)}(x)$ has the behavior for real values of x

$$G_1(x) \sim 2\pi i\begin{cases} 1 - \pi^{-1/2}x^{-3/4}\cos\left[\frac{2}{3}x^{3/2} + \frac{\pi}{4}\right] & \text{for } x \gg 1 \\ \frac{1}{3} + c_1x + \frac{c_2}{2}x^2 + \ldots & \text{for } |x| \ll 1 \\ \frac{1}{2}\pi^{-1/2}(-x)^{-3/4}\exp\left[-\frac{2}{3}(-x)^{3/2}\right] & \text{for } x \ll -1 \end{cases}$$

as indicated in Fig. 12. The constants c_1,c_2, are

$$c_1 = [1/3^{2/3}\Gamma(2/3)] = 0.35503$$
$$c_2 = [1/3^{1/3}\Gamma(1/3)] = 0.25882$$

The maximum value of $G_1(x)$ is approximately given by

$$\max\left[\frac{G_1(x)}{2\pi i}\right] \approx 1 + \frac{2(2)^{1/2}}{3\pi} = 1.3$$
$$\text{at } x = \approx \left(\frac{9}{8}\pi\right)^{2/3} = 2.32$$

In the following the same type of integral as $G_{(1)}(x,\omega_0)$ but containing a third-order pole at ω_0 will be evaluated

$$G_{(3)}(x,\omega_0) = \int_\Gamma [e^{i(x\omega-\omega^3/3)}/(\omega - \omega_0)^3]d\omega$$

Since

$$G_{(3)}(x,\omega_0) = \tfrac{1}{2}(\partial^2/\partial\omega_0)G_{(1)}(x,\omega_0)$$

the integral $G_{(3)}$ can be written in the form

$$G_{(3)}(x,\omega_0) = -\pi i\int_{-\infty}^{x}(x - s)^2\, e^{i(x-s)\omega_0}Ai[-s]ds$$

and for $\omega_0 = 0$

$$G_{(3)}(x) = -\pi i\int_{-\infty}^{x}(x - s)^2Ai[-s]ds$$

Using the differential equation defining the Airy function

$$Ai''(-s) + sAi(-s) = 0$$

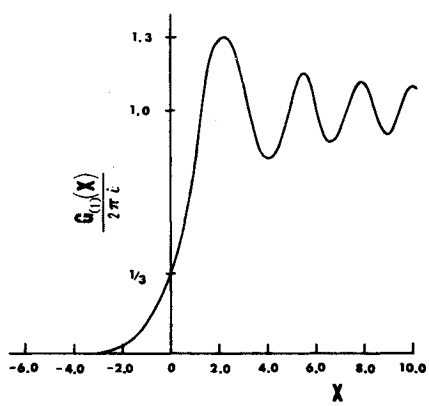

Fig. 12 The function $(1/2\pi)G_{(1)}(x)$.

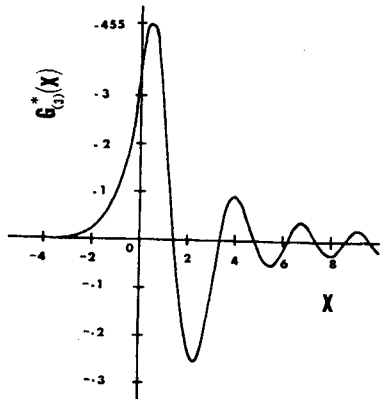

Fig. 13 The function $G^*_{(3)}(x)$.

$G_{(3)}(x)$ can be evaluated directly

$$G_{(3)}(x) = -\pi i\left\{x^2\int_{-\infty}^{x} Ai[-s]ds - xAi'[-x] + Ai[-x]\right\}$$

and has the behavior

$$G_{(3)}(x) \sim -\pi i\begin{cases} x^2 + 2\pi^{-1/2}x^{-1/4}\cos[\frac{2}{3}x^{3/2} + \pi/4] & \text{for } x \gg 1 \\ c_1 + 2c_2x + x^2/3 + \ldots & \text{for } |x| \ll 1 \\ \pi^{-1/2}(-x)^{-1/4}\exp[-\frac{2}{3}(-x)^{3/2}] & \text{for } x \ll -1 \end{cases}$$

We define the function

$$G_{(3)}{}^*(x) = \begin{cases} -x^2 - G_{(3)}(x)/\pi i & \text{for } x \geq 0 \\ -G_{(3)}(x)/\pi i & \text{for } x \leq 0 \end{cases}$$

Its behavior is shown in Fig. 13. The maximum value of $G_{(3)}{}^*(x)$ is approximately given by

$$\max[G_{(3)}{}^*(x)] \approx c_1 + \tfrac{3}{2}c_2 \approx 0.455 \quad \text{at } x \approx \tfrac{3}{2}c_2 \approx 0.388$$

References

[1] Jones, P. and Bhuta, P. G., "Response of Cylindrical Shells to Moving Loads," Vol. 31, No. 1, *Transactions of the ASME Journal of Applied Mechanics, Ser. E:* March 1964, pp. 105–111.

[2] Herrmann, G. and Baker, E. H., "Response of Cylindrical Shells to Moving Loads," Vol. 34, No. 1, *Transactions of the ASME, Ser. E: Journal of Applied Mechanics,* March 1967, pp. 81–96.

[3] Steele, C. R., "The Finite Beam With a Moving Load," *Transactions of the ASME, Ser. E: Journal of Applied Mechanics,* Vol. 34, No. 1, March 1967, pp. 111–118.

[4] Steele, C. R., "The Timoshenko Beam With a Moving Load," *Transactions of the ASME, Ser. E: Journal of Applied Mechanics,* Vol. 35, No. 3, Sept. 1968, pp. 481–488.

[5] Naghdi, P. M. and Cooper, R. M., "Propagation of Elastic Waves in Cylindrical Shells, Including the Effects of Transverse Shear and Rotatory Inertia," *Journal of the Acoustical Society of America,* Vol. 28, No. 1, Jan. 1956, pp. 56–63.

[6] Cooper, R. M. and Naghdi, P. M., "Propagation of Nonaxially Symmetric Waves in Elastic Cylindrical Shells," *Journal of the Acoustical Society of America,* Vol. 29, No. 12, Dec. 1957, pp. 1365–1373.

[7] Erdelyi, A., *Asymptotic Expansions,* Dover, New York, 1956.

[8] Van Der Waerden, B. L., "On the Method of Saddle Points," *Applied Scientific Research,* Vol. 2, Ser. B, 1951, p. 33–45.

[9] Felsen, L. B. and Marcuvitz, N., "Modal Analysis and Synthesis of Electromagnetic Fields," Research Report R-776-59 P1B-705, Oct. 1959, Air Force Cambridge Research Center.

[10] Abramowitz, M. and Stegum, I. A., *Handbook of Mathematical Functions,* U. S. National Bureau of Standards, Applied Mathematics, Ser. 55, June 1964.

[11] Steele, C. R., "Beams and Shells with Moving Loads," *Symposium on Shell Dynamics,* Aug. 1969, Western Conference of Applied Mechanics, Albuquerque.

[12] Schiffner, K. and C. R. Steele, "The Cylindrical Shell With an Axisymmetric Moving Load," SUDAAR 386, Aug. 1969, Dept. of Aeronautics and Astronautics, Stanford Univ., Stanford, Calif.